



Mössbauer Spectroscopy and X-ray Powder Diffraction Study on the Milled Gallium Oxide-hematite Nanoparticles

Monica Sorescu, Alina Foor, Jordan C. Kelly, Jennifer Aitken and Sarah Glasser

1. Duquesne University, School of Science and Engineering, Pittsburgh, PA, 15282, United States

Abstract: Samples in the milled gallium oxide-hematite nanoparticles system were synthesized by mechanochemical activation using ball milling times of 0, 2, 4, 8, and 12 hours. The specimens were characterized using Mössbauer spectroscopy and X-ray diffraction (XRD). The Mössbauer spectra were deconvoluted by least squares fitting using 2 sextets and a doublet. Lorentzian lineshapes were used in the assumption of thin absorbers approximation. The sextets were assigned to hematite and gallium-doped hematite. The relative area of doublet that represented gallium iron perovskite (gallium orthoferrite), increased with the milling time. The hyperfine magnetic fields decreased as a function of the substitution level according to the model of local atomic environment. The particle size was determined using the Scherrer method for XRPD. The crystallite dimensions were found to be in the tens of nanometers range. These structural and magnetic properties of the milled gallium oxide-hematite nanoparticles system depend on the ball milling times and molar concentrations.

Keywords: Hematite, gallium oxide, Mössbauer spectroscopy, X-ray diffraction, Nanoparticles.

INTRODUCTION

Hematite ($\alpha\text{-Fe}_2\text{O}_3$) has been in the center of several theoretical and experimental investigations due to its applications as a magnetic, semiconductor and catalytic material. Doping hematite with various transition metal and rare earth elements was found to cause an enhancement in its electrochemical and photocatalytic properties [1-6].

Gallium oxide (Ga_2O_3) is a paramagnetic compound that can be applied to functionalize hematite with multiple applications in sensing, catalysis and flexible electronics. In particular, gallium ion Ga^{3+} was determined to exhibit interesting properties when introduced in various systems. Thus, bandgap engineering of gallium oxides by crystalline disorder emerged as a future candidate for utilizations in high-power and radiofrequency electronics and deep-ultraviolet optoelectronics [7].

A comparative study of the structural, optical and electrochemical properties of $\gamma\text{-Ga}_2\text{O}_3$ synthesized by microwave hydrothermal and sol-gel techniques was accomplished in [8].

Nanoparticles have stimulated the interest of researchers in recent years, and they have been thoroughly investigated due to their numerous potential applications in biotechnology, environmental protection, data storage, magnetic sensors, and drug delivery. The properties of nanoparticles are determined by the particles' size, shape, morphology, crystallinity, surface effects, and inter-particle interactions [9].

Gallium oxide (Ga_2O_3) is an important wide bandgap transparent conductive oxide with excellent properties, which is widely used in many areas such as catalysis, electroluminescence, and biology. The research on the synthesis, properties and applications of gallium oxide nanomaterials has been developed. The preparation of gallium oxide by the hydrothermal method has been highlighted and the effects of hydrothermal conditions on the morphologies and sizes of the final products were summarized. Furthermore, the unique properties of gallium oxide in the fields of electricity, gas, heat, and biomedicine were introduced, and the excellent luminescent properties of gallium oxide were developed [10].

Gallium oxides are of wide interest due to their large bandgaps and attractive photoelectric properties. The synthesis of gallium oxide nanoparticles is based on a combination of solvent-based methods and subsequent calcination. Detailed information about solvent-based formation processes is lacking, and this limits the tailoring of materials. The formation mechanisms and crystal structure transformations of gallium oxides during solvothermal synthesis using *in situ* X-ray diffraction was accomplished in [11].

Hematite nanoparticles of average size 20 nm were produced using the sol-gel method, and the structural characterizations were performed using XRPPD and transmission electron microscopy (TEM). The XRPPD profile yielded a small fraction of the maghemite phase with hematite as a major phase. The Mössbauer spectrum was used to investigate the magnetic structure of the particles and revealed a slight non-magnetic phase and showed nanoparticles exhibiting superparamagnetism. The weighted average Morin transition temperature for the particles determined by Mössbauer is 262 K, which is remarkably similar to the bulk value [12]. The reported findings on the hematite nanoparticles will help understand the enhanced ferromagnetic behavior of the hematite nanoparticles at room temperature, which is crucial for potential applications.

A thermal reduction method has been developed to synthesize magnetite/hematite nanocomposites and pure magnetite nanoparticles targeted for different applications. The relative content of hematite $\alpha\text{-Fe}_2\text{O}_3$ and magnetite Fe_3O_4 nanoparticles in the product was accomplished by maintaining proper conditions in the thermal reduction of $\alpha\text{-Fe}_2\text{O}_3$ powder in the presence of a high boiling point solvent. The structural, electronic, and magnetic properties of the nanocomposites were studied by ^{57}Fe Mössbauer spectroscopy, XRPPD, and magnetic measurements. The content of hematite and magnetite phases was determined at every stage of the chemical and thermal treatment. It was established that not all iron ions in the octahedral B-sites of magnetite nanoparticles participate in the electron hopping $\text{Fe}^{2+} \rightleftharpoons \text{Fe}^{3+}$ above the Verwey temperature T_V . It was shown [13] that surface effects, influencing the electronic states of iron ions, dominate the vacancy effect, and thus govern the observed specific characteristics of the Verwey transition and magnetic properties. The sharp increase in coercivity observed in magnetite nanoparticles below T_V is much stronger than for bulk magnetite.

Magnetic ceramic nanoparticles system $x\text{Tm}_2\text{O}_3\text{-}(1-x)\alpha\text{-Fe}_2\text{O}_3$ ($x=0.1$ and 0.5) was synthesized by mechanochemical activation starting from hematite and thulium oxide precursors and characterized by transmission Mössbauer spectroscopy. The Mössbauer spectra were typically analyzed considering 1-3 sextets, corresponding to hematite (with and without thulium doping) and a doublet, representing thulium iron perovskite (thulium orthoferrite). The magnetic hyperfine fields (BHF) and doublet abundance were studied as

a function of BMT for both molar concentrations employed. The results were consistent with the formation of solid solutions in the investigated system. The mixed-oxide nanoparticles system has important applications in displays, sensors and photovoltaics, and for emerging utilizations related to mechanically flexible electronics [14].

Structural properties and phase composition of nanoparticles based on iron oxide were investigated. Mössbauer spectroscopy, XRPD, and scanning electron microscopy (SEM) were used for the analysis of phase transformations. According to XRPD and Mössbauer spectroscopy data, an increase in the annealing temperature, as well as the subsequent phase transformations of magnetite into maghemite and then to hematite, indicated an improvement in the structure as a result of annealing defects and vacancies. According to Mössbauer spectroscopy data at temperatures above 400°C, the typical peaks of FeO, which were characteristic for disordered iron oxide, were observed in [15]. This also confirms the improvement of the crystal structure of nanoparticles.

Spherical, mono-disperse, non-interacting iron oxide (Fe_3O_4) nanoparticles, produced by high-temperature hydrolysis of chelated iron alkoxide complexes, were investigated by Mössbauer spectroscopy. The critical diameter for room temperature superparamagnetism, an important parameter for high frequency biomedical (MRI) and IT applications, was about 11 nm. Particles of diameter 11.9 nm and greater were ferrimagnetic and showed magnetic splitting. Particles of diameter 10.6 nm and smaller were superparamagnetic and gave a non-magnetic spectrum at room temperature. The resonances narrowed as the particle size decreased and the spin relaxation rate increased. For the smallest particles (8.6 nm or less) the room temperature spectra could be resolved into two partially overlapping lines, one from the A-sites and one from the B-sites, the latter being broadened by the nuclear quadrupole interaction. Similar spectra have been previously reported for bulk Fe_3O_4 above the Curie point. The isomer shifts showed anomalies possibly arising from magnetostrictive atomic displacements [16].

Regardless of much curiosity in the fabrication and various properties of the polymorphs of gallium oxide, they were unrevealed owing to their nanoscale size and structural disorder. Convincing methods have been applied to achieve various phases of gallium oxide ($GaOOH$, α - Ga_2O_3 , β - Ga_2O_3 , γ - Ga_2O_3 , δ - Ga_2O_3 , and ε - Ga_2O_3). XRPD along with Rietveld refinement were utilized to study the structural parameters of reported phases. TEM images revealed the impact of the protocols of chemical synthesis on the morphology/size of the polymorphs of gallium oxide. Mechanistic discussion on the formation of nano-rod morphology in some of the phases ($GaOOH$ and α - Ga_2O_3) and nanoparticle morphology in other (β - Ga_2O_3 , γ - Ga_2O_3 , δ - Ga_2O_3 and ε - Ga_2O_3) phases was provided by considering the experimental parameters. The existence of Ga^{3+} ions and their local hybridization with oxygen atoms was studied in [17] using X-ray absorption spectroscopy (XAS) at the Ga K-edge and conveyed the phase dependence on the hybridization of frontier orbitals.

Magnetic ceramic nanoparticles system $xNd_2O_3-(1-x)\alpha-Fe_2O_3$ ($x=0.1, 0.3$ and 0.5) was synthesized by mechanochemical activation starting from hematite and neodymium oxide precursors and characterized by XRPD and Mössbauer spectroscopy. Rietveld refinement of XRD data evidenced the formation of neodymium orthoferrite $NdFeO_3$ as an end-product with a particle size of about 22 nm, determined using the Scherrer method for $x=0.5$. The Mössbauer spectra were typically analyzed considering 2 sextets, corresponding to hematite

and neodymium orthoferrite and a doublet, representing superparamagnetic particles (SPM). The recoilless fractions were determined using our dual absorber method and were found consistent with a decrease in particle size as a consequence of the ball milling process performed [18].

The effect of high energy ball milling on hematite for milling periods ranging from 1 to 48 h was investigated by Rietveld analysis based on XRPD patterns and Mössbauer spectroscopy. An expansion of the unit cell parameters was observed. Both Scherrer method and Rietveld analysis showed a marked decrease of the grain size with the increase of the milling time. Moreover, some dependence of the lattice parameters on the grain size was observed. Mössbauer spectroscopy measurements revealed that there were two kinds of particles which co-existed in the specimen: nanostructured and micrometric hematite. The magnetic hyperfine field was affected by the grain size [19].

Recently, the ball milling technique was key to obtaining garnet-graphene nanocomposites and crucial to determine the formation of skyrmion phase in the Fe-Co-Si system. Moreover, mechanochemical activation was used to synthesize mixed-oxide nanostructures of the type $x\text{Dy}_2\text{O}_3-(1-x)\alpha\text{-Fe}_2\text{O}_3$ with the formation of solid solutions in the system [20-24].

In the present study we shed light on the structural and magnetic properties of the $x\text{Ga}_2\text{O}_3-(1-x)\alpha\text{-Fe}_2\text{O}_3$ system with molar concentrations of $x=0.1$, 0.3, and 0.5, obtained by mechanochemical activation at different BMTs. Our investigations focused on Mössbauer spectroscopy and XRPD of the gallium oxide-hematite nanoparticles. The properties of gallium oxide-hematite nanoparticles were found to depend on BMTs and molar compositions.

MATERIAL AND METHODS

Nanoparticles of $x\text{Ga}_2\text{O}_3-(1-x)\alpha\text{-Fe}_2\text{O}_3$ ($x=0.1$, 0.3, and 0.5) were obtained by mechanochemical activation of precursor powders of hematite and gallium oxide (Alfa Aesar), with particle sizes in the tens of nanometers range. The powders were mixed manually using a mortar and pestle and introduced in a SPEX 8000 mixer mill. They were ground for time periods ranging from 0 to 12 hours. The powder to ball mass ratio was 1:5.

Transmission Mössbauer spectra were recorded at ambient temperature using a SeeCo constant accelerator spectrometer. A 25 mCi ^{57}Co gamma ray source in a Rh matrix was used. All spectra were deconvoluted by least-squares fitting using the WINORMOS package of programs in the assumption of Lorentzian line shapes. Powder XRD samples were deposited onto a zero-background silicon wafer. Data were collected using a Malvern Panalytical Empyrean 3 multipurpose X-ray powder diffractometer with an X'cellerator detector operating in Bragg-Brentano geometry and using Cu Ka radiation, $\lambda = 1.541871 \text{ \AA}$. The tube was energized using 45 kV and 40 mA. Data were collected from 5 to $100^\circ 2\theta$ in steps of 0.0167° at a scan speed of $0.023537^\circ \text{ s}^{-1}$. A 0.04 rad Soller slit and a 2° anti-scatter slit were used on the incident side of the beam, while the diffracted beam optics consisted of a 0.04 rad Soller slit, a programmable anti-scatter slit, and a nickel filter. Phase identification of crystalline components was carried out using the *X'Pert HighScore Plus* software package and the International Centre for Diffraction Data (ICDD) powder diffraction file (PDF) database.

RESULTS AND DISCUSSION

Mössbauer spectroscopy measurements were performed at room temperature in the transmission geometry to analyze the hyperfine interactions in the milled gallium oxide-hematite nanoparticles system. The mixed-oxide samples were milled for time durations of 0, 2, 4, 8, and 12 hours for molar concentrations of $x=0.1$, 0.3, and 0.5. The Mössbauer spectra of $x\text{Ga}_2\text{O}_3\text{-(}1-x\text{)}\alpha\text{-Fe}_2\text{O}_3$ for $x=0.1$ are displayed in Figure 1 (a)-(e) for milling times of 0, 2, 4, 8, and 12 hours, respectively. The Mössbauer spectra of gallium oxide-hematite nanoparticles for molar concentration of $x=0.3$ are presented in Figure 2 (a)-(e), while spectra for $x=0.5$ are given in Figure 3 (a)-(e), respectively.

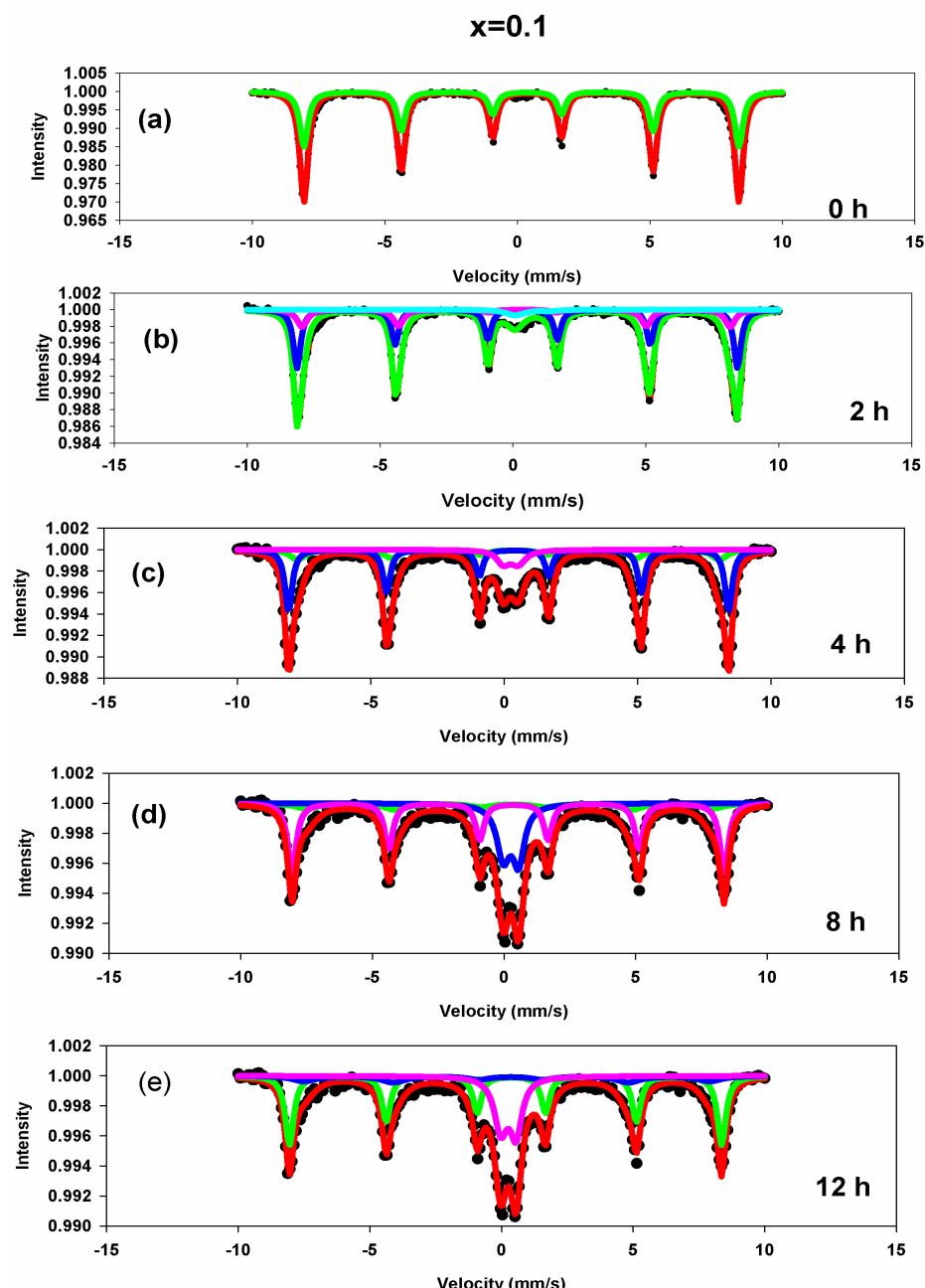


Figure 1 (a)-(e): Mössbauer spectra of gallium oxide-hematite nanoparticles for $x=0.1$ at different ball milling times, respectively.

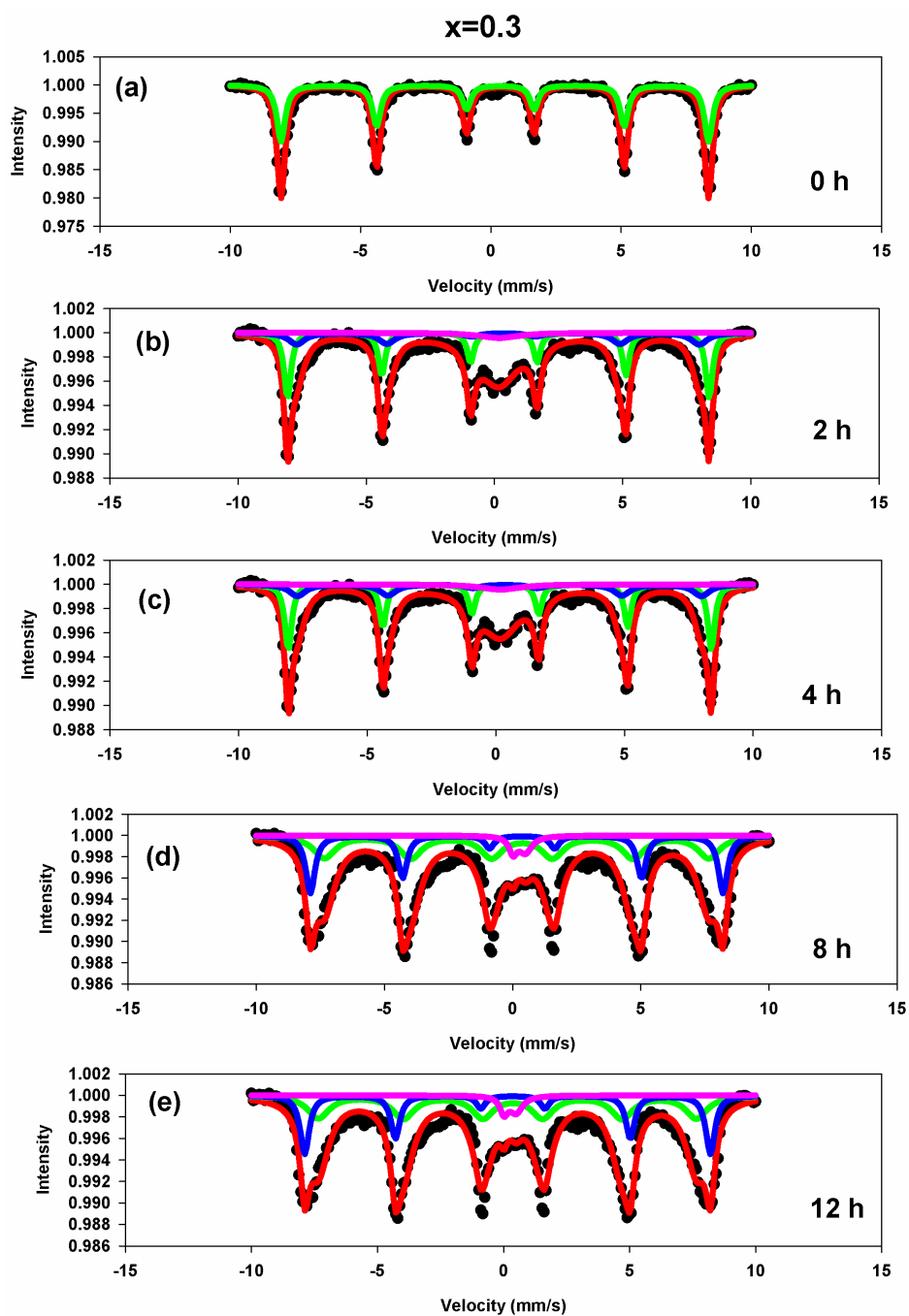


Figure 2 (a)-(e): Mössbauer spectra of gallium oxide-hematite nanoparticles for $x=0.3$ at different ball milling times, respectively.

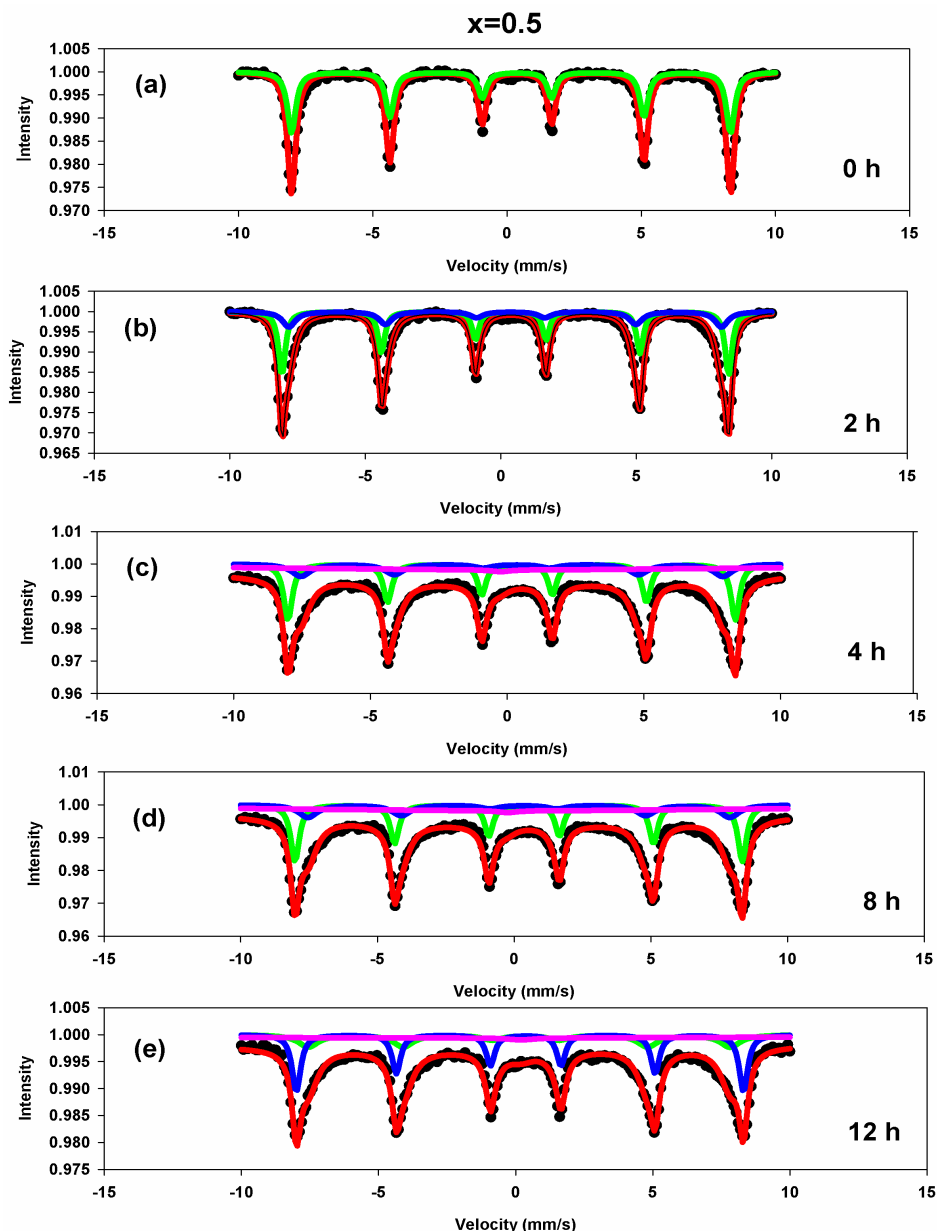


Figure 3 (a)-(e): Mössbauer spectra of gallium oxide-hematite nanoparticles for $x=0.5$ at different ball milling times, respectively.

The spectra were fitted with 2 sextets corresponding to hematite and gallium-doped hematite with hyperfine magnetic fields around 51.9 T and 48.5 T. An additional doublet was needed to obtain the best fit for the gallium oxide-hematite nanostructures. The doublet corresponds to gallium iron perovskite (gallium orthoferrite), which is a non-magnetic phase. Its intensity increases up to ~68% for $x=0.5$ and BMT=12 hours. The occurrence of the gallium iron perovskite can be understood by considering the reaction $\text{Ga}_2\text{O}_3 + \text{Fe}_2\text{O}_3 \rightarrow 2\text{GaFeO}_3$, which is believed to occur during the mechanochemical activation process.

Gallium iron perovskite production

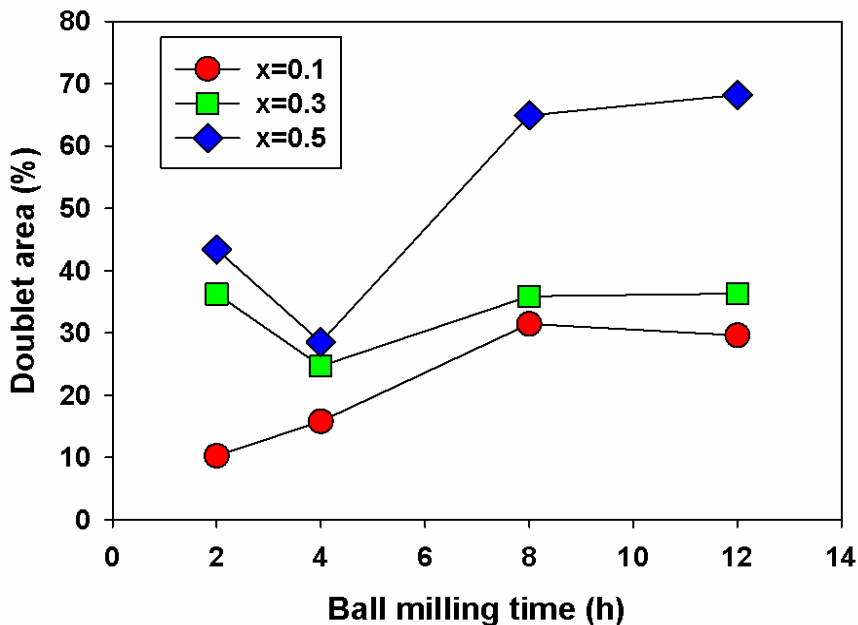


Figure 4: The doublet area (%) for gallium oxide perovskite as a function of ball milling time (h).

For pure hematite at room temperature, the magnetic hyperfine field is 51-52 T for Fe^{3+} in octahedral sites. When Ga substitutes Fe in octahedral sites, B_{hf} decreases approximately linearly with Ga content (Equation 1).

$$B_{hf}(\text{T}) \sim 49.8 - 0.12x[\text{Ga mmol mol}^{-1}] \quad (1)$$

As an example, the binomial distribution yields Equation 2:

$$P(k) = n! / [k!(n-k)!] x^k (1-x)^{n-k} \quad (2)$$

P is the probability of success and $(1-P)$ is the probability of failure. If P is close to 0, most outcomes will be near 0 successes. If P is close to 1, most outcomes will be near n successes. If $P=0.5$, the distribution is symmetric.

For $x=0.05$, $B_{hf}=49-50$ T. For $x=0.1$, $B_{hf}=48-49$ T. For $x>0.15$, $B_{hf}=46-47$ T. For $x=0.2$, $B_{hf}=46-46.5$ T; 44.5-45 T.

There is one sextet for Fe^{3+} in regular hematite lattice (higher $B_{hf} \sim 50-52$ T). The second sextet appears at Fe^{3+} near Ga substitution sites (lower $B_{hf} \sim 46-49$ T). The dependence of the B_{hf} values of these sextets on the BMTs indicates the formation of a solid solution. A higher level of substitution is not possible due to the difference in the atomic radii of the Ga^{3+} ions (130 pm) and Fe^{3+} ions (140 pm). The hyperfine magnetic fields of the sextets and the levels of substitution can be understood within the framework of the local atomic environment.

The isomer shift (δ) takes values in the range 0.2-0.4 mm/s for Fe^{3+} . The quadrupole splitting (Δ) is small, usually <0.3 mm/s.

To complement the Mössbauer results, XRD studies were performed XRPD on the gallium oxide-hematite system for molar concentration $x=0.5$. The XRD patterns are presented in Figure 5.

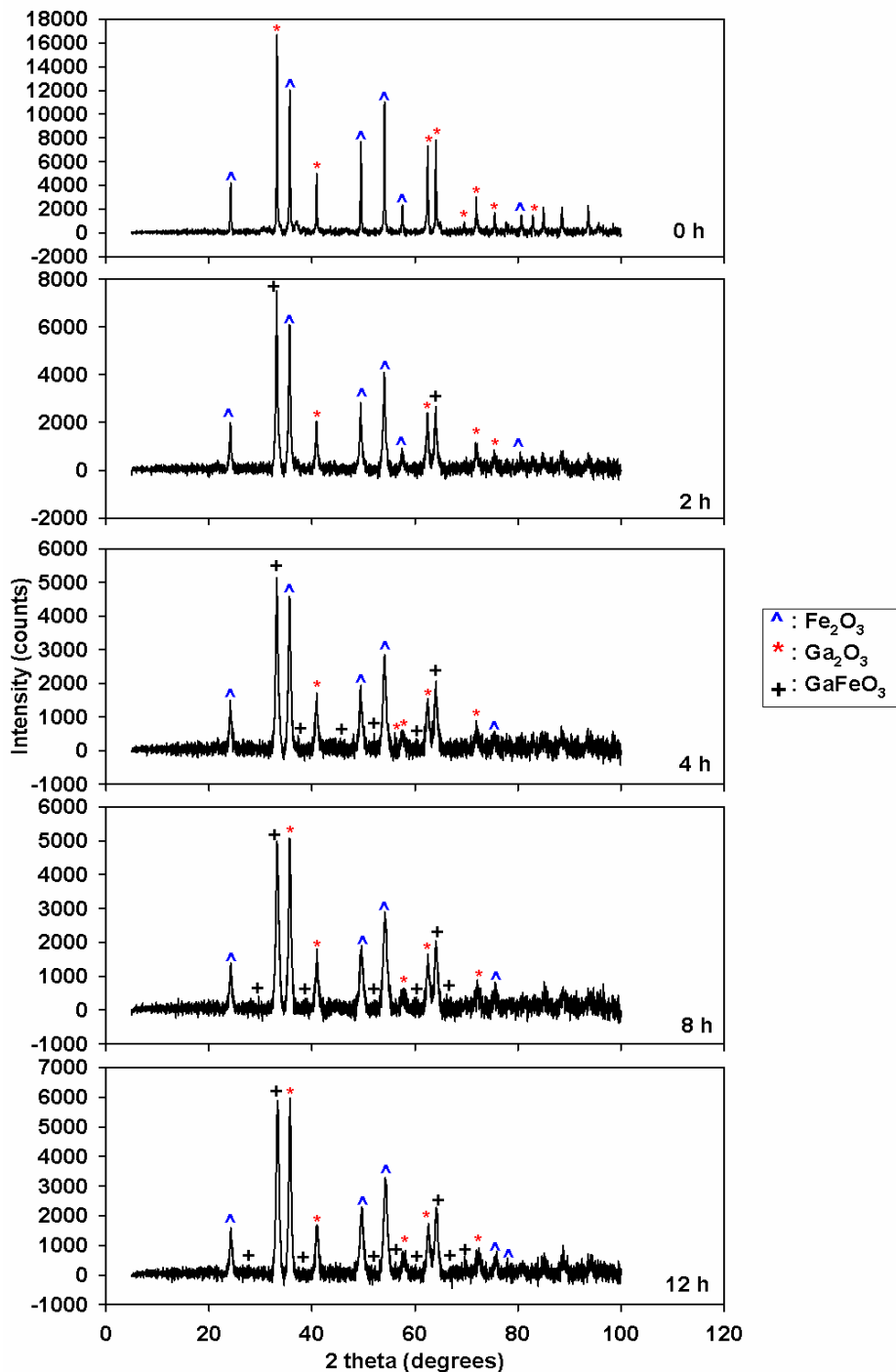


Figure 5: XRD patterns of the equimolar composition for gallium oxide-hematite nanoparticles system at different ball milling times.

At BMTs, the XRD patterns consist of peaks for hematite and gallium oxide. They were identified using the PDF cards: 01-089-0598 (Fe_2O_3) and 01-087-1901 (Ga_2O_3). At high BMTs, the XRD patterns were dominated by the resonances of the gallium iron perovskite, GaFeO_3 .

(PDF card: 01-076-1005). These results are in good, qualitative agreement with the Mössbauer findings presented in the previous section.

To determine the particle size from XRD patterns, the Scherrer method was used for the most intense (104) peak. For this equation, the dimension (D) of the crystallites is given by Equation 3:

$$D = K\lambda / \beta \cos\theta \quad (3)$$

In this equation, $K=0.94$, $\lambda=1.54 \text{ \AA}$, $\beta(\text{rad})=0.003080506$.

For 0 h, $D=46.99 \text{ nm}$; for 2 h, $D=47.02 \text{ nm}$; for 4 h, $D=47.03 \text{ nm}$; for 8 h, $D=47.05 \text{ nm}$; and for 12 h, $D=47.11 \text{ nm}$. It can be seen that θ increases with BMT, $\cos\theta$ decreases and D slightly increases with milling time. This result could be due to agglomerations of particles. Overall, the crystallite dimensions are in the tens of nanometers range. These structural and magnetic properties of the milled gallium oxide-hematite nanoparticles system depend on the BMTs and molar concentrations.

CONCLUSION

We synthesized the $x\text{Ga}_2\text{O}_3\text{-}(1-x)\alpha\text{-Fe}_2\text{O}_3$ system by mechanochemical activation using the ball milling technique for time durations of 0-12 hours and for molar concentrations $x=0.1$, 0.3 , and 0.5 . The structural and magnetic properties of the gallium oxide-hematite nanoparticles system were characterized using Mössbauer spectroscopy and XRPD measurements. The Mössbauer spectra were analyzed using 2 sextets and one doublet, where the sextets correspond to hematite and gallium-doped hematite, and the doublet was assigned to gallium iron perovskite, whose intensity increases with ball milling time. The phase assignment was confirmed by XRD. The particle size was determined using the Scherrer method and found to be in the tens of nanometers range. These structural and magnetic properties of the milled gallium oxide-hematite nanoparticles system depend on the BMTs and molar concentrations. This work represents a viable synthetic avenue toward gallium doped hematite nanostructure for spintronic applications.

ACKNOWLEDGMENT

This work was supported in part by the National Science Foundation, USA under grants number DMR-0854794 and DMR-1002627-1. J.A. and J.K. acknowledge the support of the National Science Foundation, USA under grant DMR-1611198.

CONFLICTS OF INTEREST

There are no conflicts of interest regarding the work described in this paper.

REFERENCES

- [1]. Rozenberg, G., et al., *High pressure structural studies of hematite*. Physical Review B, 2002. 65: p. 064112.

- [2]. Bergenmayer, W., et al., *Ab Initio thermodynamics of oxide surfaces: Oxygen on hematite (0001)*. Physical Review B, 2004. 69: p. 195409.
- [3]. Zheng, Y., et al., *Quasicubic hematite nanoparticles with excellent catalytic performance*. Journal of Physical Chemistry, 2006. 110: p. 3093-3097.
- [4]. Wu, C., et al., *Synthesis of hematite nanorods: Diameter-size and shape effects on their applications in magnetism, lithium ion battery, and gas sensors*. Journal of Physical Chemistry, 2006. 110: p. 17806-17812.
- [5]. Liu, J.Z., *Morin transition in hematite doped with Iridium ions*. Journal of Magnetism and Magnetic Materials, 1986. 54-57: p. 901-902.
- [6]. Stroh, C., et al., *Ruthenium oxide-hematite magnetic ceramic nanostructures*. Ceramics International, 2015. 41: p. 14367-14375.
- [7]. Jewel, M.U., et al., *A comprehensive study of defects in gallium oxide by density functional theory*. Computational Materials Science, 2023. 218: p. 111950.
- [8]. Falkova, A.N., et al., *Mechanoactivated interaction of hematite and gallium*. Journal of Alloys and Compounds, 2009: p. 31-34.
- [9]. Ho, Y.C., et al., *Deep ultraviolet optical anisotropy of gallium oxide thin films*. ACS OMEGA, 2024: p. 27963-27968.
- [10]. Singh, A., et al., *Intra- and inter-conduction band optical absorption processes in gallium oxide*. Applied Physics Letters, 2020: p. 072103.
- [11]. Gilbert, B., et al., *Band-gap measurements of bulk and nanoscale hematite by soft-ray spectroscopy*. Physical Review B, 2009: p. 035108.
- [12]. Krehula S., et al., *Synthesis and microstructural properties of mixed iron-gallium oxides*. Journal of Alloys and Compounds, 2015: p. 130-141.
- [13]. Irshad, I., et al., *Tuning of magnetic and dielectric properties of gallium doped hematite nanospheres*. Journal of Alloys and Compounds, 2024: p. 173901.
- [14]. Cho, S., et al., *New luminescent band due to nitrogen impurities in gallium oxide powders*. Materials Letters, 2012: p. 1004-1009.
- [15]. Jubu, P.R., et al., *Optical and optoelectronic properties of gallium oxide films fabricated by the chemical vapor deposition method*. Physica B: Condensed Matter, 2024: p. 415763.
- [16]. Jubu, P.R., et al., *Enhanced red shift in optical absorption edge and photoelectrochemical performance of N-incorporated gallium oxide nanostructures*. Vacuum, 2020: p. 109704.
- [17]. Ho, Y.C., et al., *Deep ultraviolet optical anisotropy of gallium oxide thin films*. ACS OMEGA, 2024: p. 27963-27968.
- [18]. Singh, A., et al., *Intra- and inter-conduction band optical absorption processes in gallium oxide*. Applied Physics Letters, 2020: p. 072103.
- [19]. Glasser, S., et al., *Effects of mechanochemical activation on the structural, magnetic and optical properties of yttrium iron garnet-graphene nanoparticles*. Physica B, 2023. 650: p. 414501.
- [20]. Sorescu, M., et al., *Formation of skyrmion phase in the Fe-Co-Si system by mechanochemical activation*. Physica B, 2024. 688: p. 416153.
- [21]. Glasser, S., et al., *Synthesis and characterization of gadolinium oxide-hematite magnetic ceramic nanostructures*. Journal of Minerals and Materials Characterization and Engineering, 2023. 11: p. 1-15.

[22]. Sorescu, M., et al., *Mechanochemical synthesis and Mössbauer characterization of neodymium oxide-hematite magnetic ceramic nanoparticles: Phase sequence and recoilless fraction*. Materials Chemistry and Physics, 2022. 277: p. 125511.

[23]. Diamandescu, L. et al., *Multifunctional $GaFeO_3$ obtained via mechanochemical activation followed by calcination of equimolar nanosystem gallium oxide-hematite*. Nanomaterials, 2021. 11: p.57.

[24]. Diaz-Guerra, C., et al., *Magnetic transitions in hematite nanowires*. Journal of Applied Physics, 2009. 106: p. 104302.